

Rapidly sintering nanosized SiC particle reinforced TiC composites by the spark plasma sintering (SPS) technique

LIANJUN WANG, WAN JIANG*, LIDONG CHEN

The State Key Laboratory of High Performance Ceramics and Superfine Microstructure, Shanghai Institute of Ceramics, Chinese Academy of Sciences, 1295 Dingxi Road, Shanghai 200050, People's Republic of China

E-mail: wanjiang@mail.sic.ac.cn

Different content of nanosized SiC reinforced TiC matrix composites were fabricated at 1600°C by spark plasma sintering (SPS) without any aids. It was found that the materials could be sintered in a relatively short time (12 min) and low sintering temperature (1600°C) to satisfactory relative density (99%). The phase distribution and microstructure of composites have been investigated by optical microscopy and scanning electron microscope. Fracture toughness and Vickers hardness at room temperature were also measured by indentation tests. The results showed that nanosized SiC particles addition could inhibit the coalescence of TiC grains and increase fracture toughness of composites due to the crack deflections. © 2004 Kluwer Academic Publishers

1. Introduction

Titanium carbide is an attractive material for wear and structure applications because of its high melting point, extreme hardness and excellent chemical stability [1–3]. However, TiC ceramics have low sinterability and toughness, which limit their use under severe stress [4]. Particle or whisker reinforcement is a promising method to overcome the brittleness [5, 6]. Unfortunately, a drawback to the use of whiskers is that the whiskers are potential health hazards [7]. TiC ceramics can be toughened and strengthened with the addition of particles, such as SiC, TiN [3, 6, 8, 9]. A few reports have showed that TiC/SiC ceramic-matrix composites have superior properties compared with monolithic TiC and SiC ceramic [1–3, 8]. Recently, several investigations have demonstrated that nano-composites, in which the nano-size dispersoids are incorporated within the matrix grains and at the grain boundaries, exhibit significantly improved mechanical properties [6, 10, 11]. The nanometer-size dispersoids effectively restrain the growth of matrix gains or change the fracture mode from transgranular to intergranular [11].

The highly covalently bonded nature of TiC and SiC in TiC-SiC composites makes sintering difficult without the use of sintering aids [4]. To date, TiC-SiC composites have been prepared by hot-pressing or pressureless sintering with the aid of C and Al or Al₂O₃ and Y₂O₃ to near full density at temperatures ranging from 1850 to 2000°C, although low temperature sintering is more economical [12–14]. But the relatively low melting point of sintering aids limits the application of these

TiC-SiC composites at higher temperature. So it is significant to consolidate TiC-SiC composites without applying sintering aids.

Recently, rapid sintering techniques, spark plasma sintering (SPS) that can enhance sintering and reduce the time available for grain growth, and also high pressure sintering, has been used for processing of ceramics and metallic materials, for example: Si₃N₄, Si₃N₄-SiC, Ti₃SiC₂, (TiWCr)B₂ etc. [15–19]. Unlike the conventional sintering method (hot-press), it is believed that metals and ceramics can be rapidly sintered using SPS at a relatively lower temperature and short time.

In this paper, we reported a novel processing route (SPS) to fabricate nano-SiC reinforced TiC composites without any sintering aids at 1600°C, and at the same, we investigated the effect of the addition of nano-SiC particles on microstructure and mechanical properties of TiC composites.

2. Experimental procedure

This work was conducted by using commercially available powders of TiC ($d = \sim 1.5 \mu\text{m}$, 99%, The Mineralogical Society of Japan), nano-SiC ($d = \sim 100 \text{nm}$, 99%, Hefei kiln nanometer technology development Co. Ltd). Nano-SiC powder was dispersed by using an ultrasonic device and the nano-SiC and TiC were mixed with different ratios of TiC/SiC in a ball mill in ethanol together with silicon carbide balls for 24 h. After drying and sieving, the mixed powders were put into

*Author to whom all correspondence should be addressed.

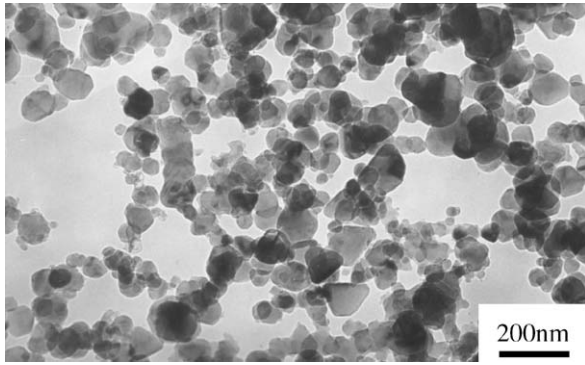


Figure 1 TEM micrograph of SiC powders.

a graphite die (15 mm in diameter) and sintered with Dr. Sinter[®] 2040 spark plasma sintering system (Sumitomo Coal Mining Co., Tokyo, Japan) in vacuum (less than 4 Pa). The heating rate was controlled in the range

of 100–200°C/min and the pressure was applied from 1000°C and maintained constant at 70 MPa. The temperature was held at 1600°C for 1 min before turning off the power.

After sintering, the surfaces of samples were ground to remove the graphite layer, then were polished with different particle size (from 3.5–0.5 μm) diamond paste. The phase distribution of the polished samples were performed using optical microscopy (Model BX51M, Olympus Optical, Tokyo, Japan). The densities of consolidated specimens were obtained using the Archimedes immersion method with deionized water as the immersion medium. The theoretical densities of the specimens were calculated according to the rule of mixtures. Microstructural observation was conducted using an scanning electron microscope (EPMA, 8705QH₂, Shimadzu, Japan). Indentation tests were performed with a diamond Vickers indenter. The indentation

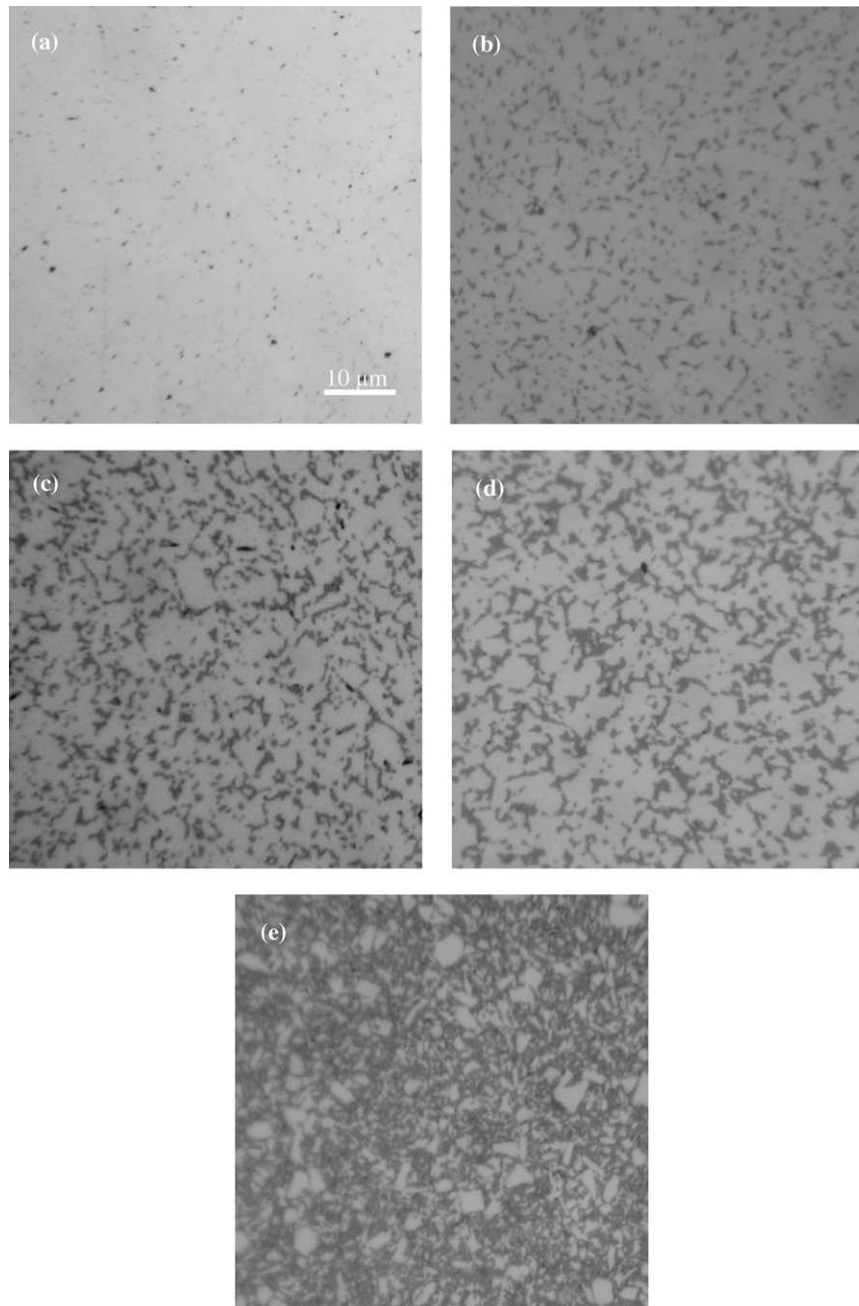


Figure 2 Optical microscope observation of samples sintered by SPS at 1600°C for 1 min: (a) monolithic TiC; (b) TiC-10wt%SiC; (c) TiC-20wt%SiC; (d) TiC-30wt%SiC, and (e) TiC-40wt%SiC composites.

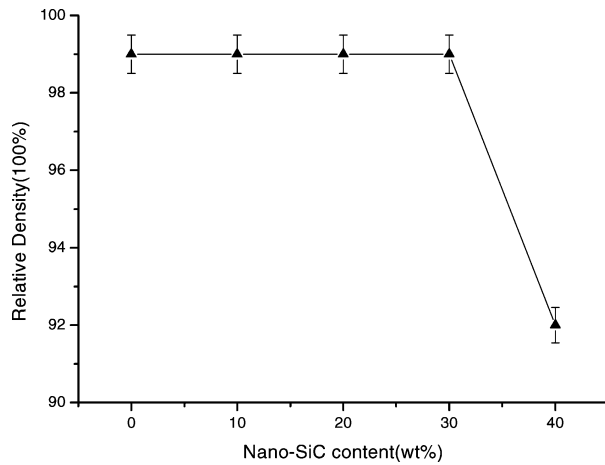


Figure 3 Variation of relative density of sintering samples with content of SiC.

parameters for fracture toughness (K_{IC}) at room temperature and Vickers hardness measurements were made using a 10 kg loads with a dwell of 15 s. The fracture toughness was calculated according to Ref. [20].

3. Experimental results

Fig. 1 shows the morphology of nano-SiC particles used as starting materials in the present work. From the Fig. 1, it can be seen that the average diameter of a nano-SiC particle is ~ 100 nm. Fig. 2 is optical micrographs of the polished surface of the monolithic TiC and nano-SiC/TiC composites at 1600°C , 70 MPa for 1 min without any sintering aid. The gray phase is the TiC, and the dark phase is the SiC in the Fig. 2. As shown, the composites are two-phase particulate composites consisting of uniformly distributed small agglomerated SiC particles in the TiC matrix. The cluster of the nanosized SiC grows bigger and gradually deviate from sphere with the increase of nano-SiC content. When the nanosized SiC content reaches 20 wt%, SiC forms certain constituent phase and the compos-

ites have a network microstructure. When nanosized SiC content reaches 40 wt%, the distribution of TiC changes from continuous phase to isolated phase because of the greater probability of clustering of SiC particles as amount of addition is increased.

Fig. 3 shows the variations of the relative density of composites with nano-SiC content under same conditions, 1600°C with 70 MPa and the soaking time of 1 min. For monolithic TiC, TiC-10wt%SiC, TiC-20wt%SiC and TiC-30wt%SiC, the relative density in excess of 99% was achieved at 1600°C . However, in the case of TiC-40wt%SiC, relative density corresponding to 92% at same sintering conditions (1600°C with 70 MPa and the soaking time of 1 min) due to inherent low sinterability and high content of SiC.

The changes in fracture toughness and Vickers hardness with the weight fraction of reinforcing particles are shown in Fig. 4. Fracture toughness initially increased with the content of SiC and reached a maximum value of $5.76 \text{ Mpa} \cdot \text{m}^{1/2}$ at 20 wt% reinforcing SiC particles. The value is approximately 90% higher than that of monolithic TiC. The increase in fracture toughness can be attributed to the deflection of cracks due to dispersion of different particles, as shown in Fig. 5. The Vickers hardness of composites increased with the content of SiC, and showed a maximum value at TiC-30wt%SiC sample but not at TiC-40wt%SiC sample. It is attributed to the low relative density (92%) of TiC-40wt%SiC sample.

Fig. 6 shows the fracture surfaces of monolithic TiC and TiC-20wt%SiC composite. For the monolithic TiC (as shown in Fig. 6(a)), fracture mode is mostly transgranular, but the fracture mode of TiC-20wt%SiC composite is intergranular mainly. The fracture surface of the TiC-20wt%SiC composite was investigated and done spot analyses by energy dispersive spectroscopy, and the results showed fine grains were SiC, and coarse grains were TiC. When the crack propagates forward and reaches the SiC particles distributed at the boundaries of TiC grains, it is difficult for the crack to cross

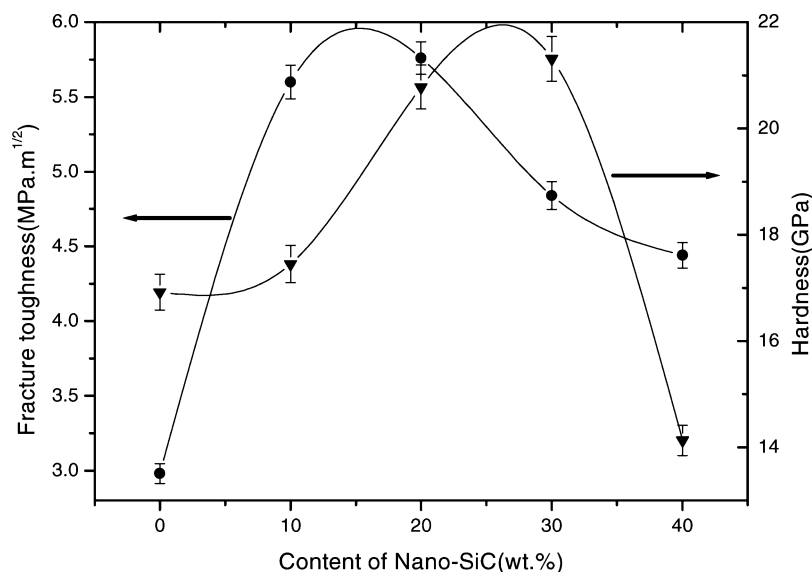


Figure 4 Variation of the fracture toughness and Vickers hardness of TiC-SiC composites with nanosized SiC content (1600°C , 1 min without any sintering aids).

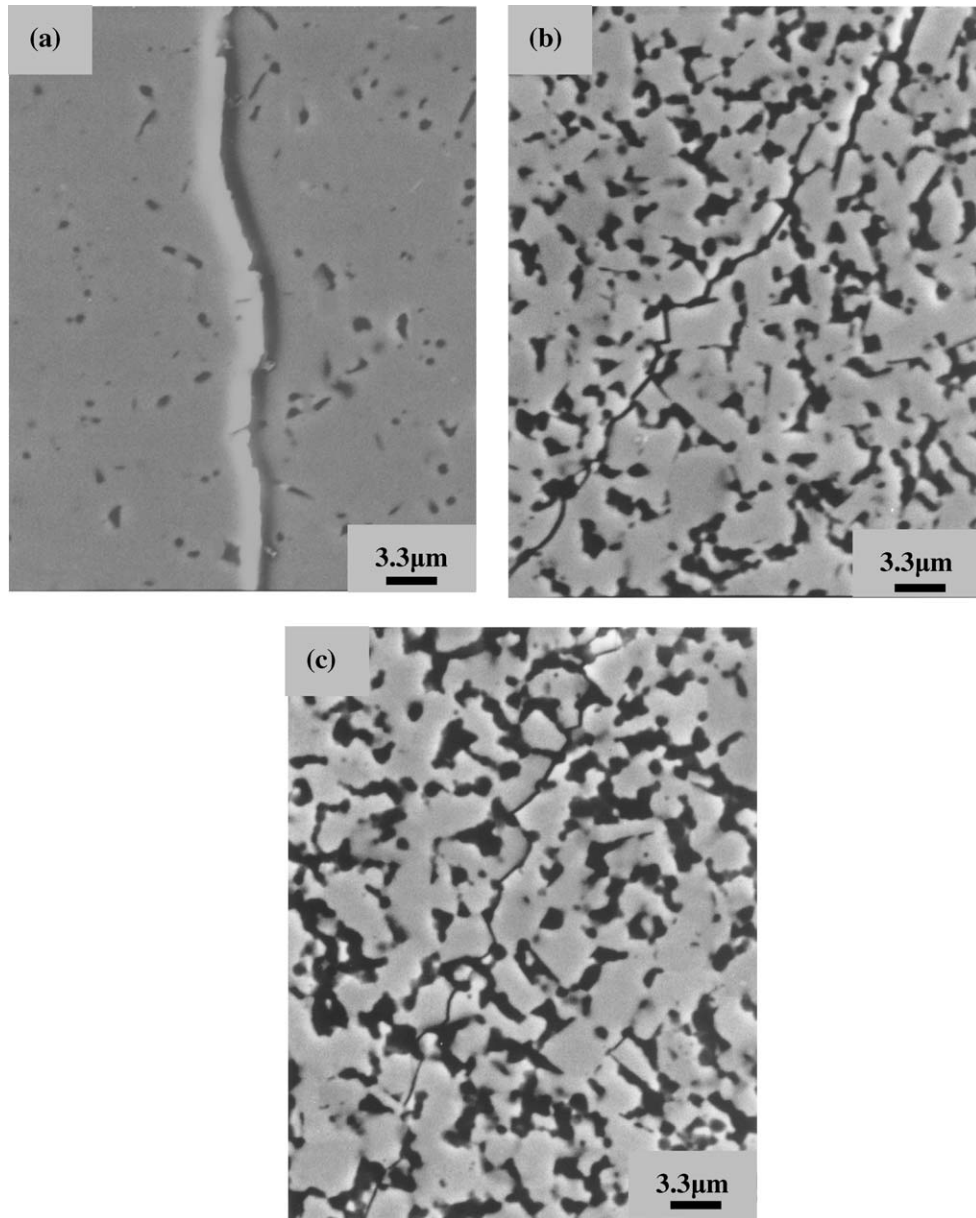


Figure 5 Scanning electron micrographs of a crack path induced by a Vickers' indenter in (a) monolithic TiC; (b) TiC-20wt%SiC; and (c) TiC-30wt%SiC.

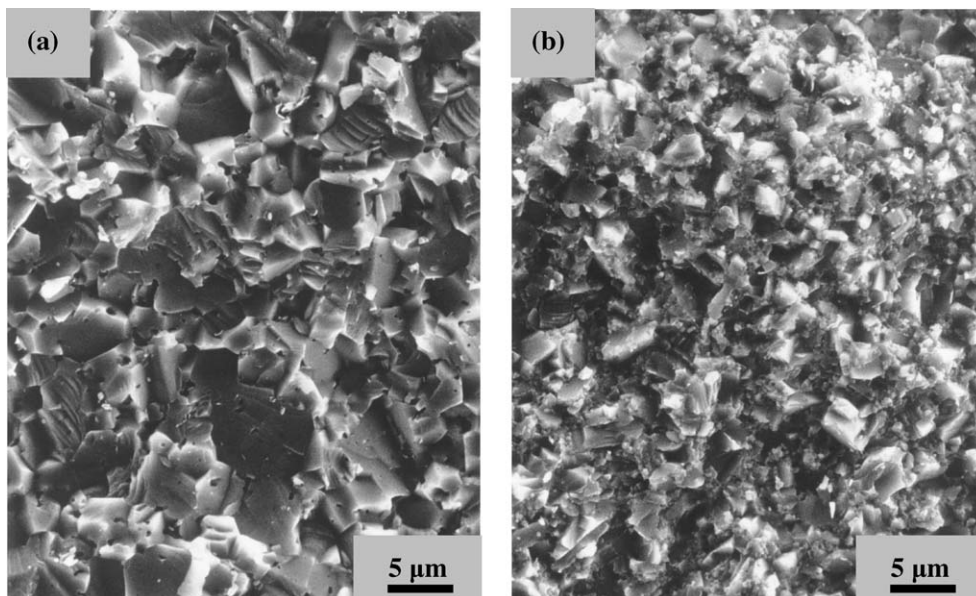


Figure 6 SEM micrographs of fracture surface of (a) monolithic TiC and (b) TiC-20wt%SiC.

through the SiC particles and the crack will deflect and propagate along the TiC and SiC grains boundaries, as shown in Fig. 5. Therefore, the value of fracture toughness increased due to changing fracture mode and showed a maximum value of $5.76 \text{ MPa} \cdot \text{m}^{1/2}$. In addition, the adding nanosized SiC particles to TiC matrix can prevent evidently the coalescence of TiC grains, as shown in Fig. 6.

4. Conclusion

The high dense TiC composites containing 0, 10, 20, 30 and 40 wt% nanosized SiC were fabricated at 1600°C by SPS without any sintering aids. The effect of nanosized SiC particles dispersoids on the fracture toughness of composites was investigated. Adding nanosized SiC particles to TiC matrix increased the room temperature fracture toughness of composites and inhibited the coalescence of TiC grains.

Acknowledgements

The authors wish to acknowledge with thanks supports of this research by the Natural Science Foundation of China (No 50232020).

References

1. G. C. WEI and P. F. BECHER, *J. Amer. Ceram. Soc.* **67** (1984) 571.
2. KYEONG-SIK CHO, YOUNG-WOOK KIM, HEON-JIN CHOI and JUNE-GUNN LEE, *ibid.* **79** (1996) 1711.
3. H. ENDO, M. UEKI and H. KUBO, *J. Mater. Sci.* **26** (1991) 3769.

4. DONGLIANG JIANG, "Fine Ceramics Materials [M]" (Chinese Substance Press, Beijing, 2000) p. 169.
5. A. KAMIYA, K. NAKANO and A. KONDOH, *J. Mater. Sci. Lett.* **8** (1989) 566.
6. N. LIU, Y. D. XU, H. LI, G. H. LI and L. D. ZHANG, *J. Eur. Ceram. Soc.* **22** (2002) 2409.
7. G. M. SONG, Q. LI, G. W. WEN and Y. ZHOU, *Mater. Sci. Eng. A* **326** (2002) 240.
8. H. ENDO, M. UEKI and H. KUBO, *J. Mater. Sci.* **25** (1990) 2503.
9. KYEONG-SIK CHO, HEON-JIN CHOI, JUNE-GUNN LEE and YOUNG-WOOK KIM, *J. Mater. Sci. Lett.* **17** (1998) 1081.
10. MASATO UEHARA, HIROFUMI OGATA, HIDEAKI MAEDA and JUNICHI HOJO, *J. Jap. Soc. Powd. Metal.* **45** (1998) 1166.
11. K. W. CHAE, K. NIARA and D. Y. KIM, *J. Mater. Sci. Lett.* **14** (1995) 1332.
12. M. A. JANNEY, *Am. Ceram. Soc. Bull.* **65** (1986) 357.
13. D. L. JIANG, J. H. WANG, Y. L. LI and L. T. MA, *Mater. Sci. Eng. A* **109** (1989) 401.
14. YOUNG-WOOK KIM, SUN-GU LEE and YOUNG-IL LEE, *J. Mater. Sci.* **35** (2000) 5569.
15. ZHIJIAN SHEN, ZHE ZHAO, HONG PENG and MATS NYGREN, *Nature* **417** (2002) 266.
16. D. S. PERERA, M. TOKITA and S. MORICCA, *J. Eur. Ceram. Soc.* **18** (1998) 401.
17. JULIN WAN, MATTHEW J. GASCH and AMIYA K. MUKHERJEE, *J. Amer. Ceram. Soc.* **86** (2003) 526.
18. Z. F. ZHANG, Z. M. SUN, H. HASHIMOTO and T. ABE, *J. Eur. Ceram. Soc.* **22** (2002) 2957.
19. HISASHI KAGA, ELLEN M. HERIAN and ZUHAIR A. MUNIR, *J. Amer. Ceram. Soc.* **84** (2003) 2764.
20. JIANLIN LI, DONGLIANG JIANG and SHOU-GONG TAN, *J. Europ. Ceram. Soc.* **22** (2002) 551.

Received 14 July 2003

and accepted 12 March 2004